Energy & Environmental Science

Cite this: *Energy Environ. Sci.*, 2012, **5**, 7898

www.rsc.org/ees

COMMUNICATION

Triple-coaxial electrospun amorphous carbon nanotubes with hollow graphitic carbon nanospheres for high-performance Li ion batteries†

Yuming Chen,[a] Zhouguang Lu,[a] Limin Zhou,*[a] Yiu-Wing Mai[ab] and Haitao Huang[c]

Received 23rd February 2012, Accepted 30th April 2012
DOI: 10.1039/c2ee22085g

We prepared amorphous carbon nanotubes decorated with hollow graphitic carbon nanospheres (ACNHGCNs) using a novel triple-coaxial electrospinning method and characterized the electrochemical performance of these ACNHGCNs as anode materials for lithium ion batteries (LIBs). The ACNHGCNs displayed a very high reversible specific capacity of ~969 mA h g^{-1} at a current density of 50 mA g^{-1}, which is nearly 2.6 times the theoretical capacity of graphite (372 mA h g^{-1}). The ACNHGCNs also showed a high volumetric capacity of ~1.42 A h cm^{-3} and good cycling stability and outstanding rate capability. The prepared ACNHGCNs can be a promising alternative anode material used for high-energy, low-cost and environmentally friendly lithium ion batteries.

Considerable attention has been paid to rechargeable lithium ion batteries (LIBs) because of their high energy density and long cycle lifetime.[1] However, exploring and developing novel electrode materials with sufficiently high energy and power density to meet the requirements imposed on application of LIBs in high-power devices such as electric vehicles (EV) and hybrid electric vehicles (HEV) remains a challenge. The current commercially available anode materials employed in LIBs are graphites due to their long lifespan, low cost and low electrochemical potential with respect to lithium metal.[2] However, the practical use of carbon in the application of LIBs in EV and HEV has been restricted by its low storage capacity (372 mA h g^{-1} of graphite corresponding to a stoichiometric LiC_6 composition) due to the structure of graphite, and the limited rate performance of the rate-limiting step in the chemical diffusion of lithium ions within the bulk electrode material.[3,4] Moreover, the unwanted metallic lithium plating inevitably occurs on the graphite-based anode because of its working potential of around 0 V *versus* Li^+/Li. This destroys the solid electrolyte interface (SEI) on the graphite surface, decreases cycling efficiency and raises safety issues due to the internal short-circuiting associated with the formation of dendritic lithium.[5,6] In addition, graphite-based anode materials have a very flat charge–discharge plateau at around 0.3 V which makes it difficult to predict the state of charge and discharge of the batteries. To address these problems, intensive research has been devoted to exploring novel carbonaceous-based anode alternatives such as 1-D carbon nanofibers and nanotubes,[7,8] 2-D carbon nanosheets[9] and graphenes possessing a broad operating potential range about 0–3 V and sloping charge–discharge characteristics.[10] But, the high storage capacity of these materials remains an issue. Recently, hybrid carbon nanomaterials and graphene nanostructures have been shown to be promising candidates for anodes in LIBs. These nanostructures can lead to multiple functionalities by creating additional sites for storage of lithium ions, which can improve considerably the lithium storage capacity.[11–14] However, their potential application in practical LIBs is hindered by their limited cycle life, resulting from the volume expansion during the repeated lithiation and delithiation processes.[13,14]

To develop LIBs with a large capacity and long lifetime, novel anode materials need to be developed. In this study, we have fabricated a novel architecture made of amorphous carbon nanotubes decorated with hollow graphitic carbon nanospheres (ACNHGCNs)

[a]*Department of Mechanical Engineering, The Hong Kong Polytechnic University, Hong Kong, China. E-mail: mmlmzhou@inet.polyu.edu.hk; Fax: +86 852-2365 4703; Tel: +86 852-2766 6663*
[b]*Centre for Advanced Materials Technology (CAMT), School of Aerospace, Mechanical and Mechatronics Engineering J07, The University of Sydney, NSW 2006, Australia*
[c]*Department of Applied Physics and Materials Research Center, The Hong Kong Polytechnic University, Hong Kong, China*

† Electronic supplementary information (ESI) available: Synthetic details and additional experimental data. See DOI: 10.1039/c2ee22085g

Broader context

A novel architecture consisting of amorphous carbon nanotubes decorated with hollow graphitic carbon nanospheres (ACNHGCNs) has been prepared by using a triple-coaxial electrospinning method. The ACNHGCNs displayed a very high reversible specific capacity of ~969 mA h g^{-1} and a volumetric capacity of ~1.42 A h cm^{-3}, good cycling stability, and outstanding rate capability. The prepared ACNHGCNs can be a promising alternative anode material used for high-energy, low-cost and environmentally friendly lithium ion batteries.

by a novel triple-coaxial electrospinning method in combination with subsequent calcination and acid treatment, and have extensively characterized their electrochemical performance as high-performance anode materials for next-generation high energy and high power LIBs. Compared with the amorphous carbons, the ACNHGCNs provide additional sites for storage of lithium ions, thus improving the lithium-storage capacity. The special structure of ACNHGCNs provides a buffer to alleviate the volume expansion caused by repeated Li^+ intercalation, which enhances the cycle lifetime.[15] Due to the highly graphinized hollow carbon nanospheres that have been well-dispersed throughout the amorphous carbon nanotubes, ACNHGCNs possess high electronic conductivity and facilitate fast Li^+ diffusion inside the electrode so that very good rate capability can be achieved.[16–18] We have also demonstrated that electrospinning is a simple and elegant method to produce novel carbon nanostructures with superior electro-chemical properties.

A typical triple-coaxial electrospinning method schematically is illustrated in Fig. 1a. Three viscous liquids were simultaneously fed through the inner (mineral oil), middle (polyacrylonitrile (PAN) solution), and outer (a mixed solution of polyvinyl pyrrolidone (PVP) and nickel acetate ($Ni(Ac)_2$)) metallic capillaries, where PAN served as the carbon source, nickel formed by the decomposition of $Ni(Ac)_2$ as a normal catalyst for graphitization of carbon,[19,20] and PVP as a template. When a suitable high voltage of 17 kV was applied between the spinneret and the collector, the jet was stretched by electrostatic forces. PVP and PAN were mixed together during the electrospinning process due to the use of the same DMF solvent. Hence, $Ni(Ac)_2$ could be uniformly transported onto the surface and the PAN matrix.[21] Finally, coaxial composite nanofibers were fabricated. Subsequently, as described in Fig. 1b, the collected nanofibers were stabilized at 250 °C for 2 h under H_2 (5%)/N_2 (95%) to evaporate the oil to form a nanotube structure. After calcining at 600 °C for 3 h under a H_2/N_2 atmosphere, PVP was burnt out and a highly porous structure was formed and Ni nanoparticles were produced by the decomposition of $Ni(Ac)_2$. The PAN coated on the Ni nanoparticles was decomposed into amorphous carbon, which was then transformed to graphitic carbon under the catalytic effect of Ni metal nanoparticles. As a result, amorphous carbon nanotubes decorated with Ni nanoparticles encapsulated in graphitic carbon nano-spheres (ACNNNGCNs) were fabricated. After immersion in HCl solution, the Ni nanoparticles were dissolved to produce ACNHGCNs. Triple-coaxial electrospinning was used to prepare the ACNHGCNs rather than coaxial electrospinning for two main reasons. First, in the precursor, the addition of more $Ni(Ac)_2$ into the PAN solution not only greatly increased the electrospinning solution conductivity, which led to deep atomization of the liquids and their breakage into polydispersed electrosprays,[22] it also allowed the mixed PAN–$Ni(Ac)_2$ solution to act as an outer fluid precipitate when the concentration of $Ni(Ac)_2$ was raised to ~11 wt%. The higher the concentration of $Ni(Ac)_2$, the better the performance, because the reduced metallic Ni nanoparticles are crucial catalysts for the formation of hollow graphitic carbon nanospheres. Second, introducing PVP into the PAN–$Ni(Ac)_2$ solution increased the number of functional groups for Ni coordination to avoid the precipitation of $Ni(Ac)_2$. During the calcination of PVP/PAN/$Ni(Ac)_2$@Oil composite fibers, PVP was burnt out and PAN turned into carbon. The concentration of Ni formed by decomposing $Ni(Ac)_2$ was increased in the carbon matrix. Further, this method prevents the formed Ni from aggregating and controlling the diameter of the hollow graphitic carbon nanospheres obtained by post-treating Ni with acid, which plays a very important role in the electrochemical performance of the prepared materials. However, phase separation between PAN and PVP did occur in the PAN/PVP/$Ni(Ac)_2$ electrospun solution due to the limited solubility of these compounds. The field-emission scanning electron microscopy image (FESEM) in Fig. 2a reveals the presence of some nanospheres (diameter ≈ 25 nm) on the surface of the nanotubes having an average outside diameter of 200 nm. At the same time, nanospheres were observed on the surface of the inside wall of the broken nanotubes (see arrow in Fig. 2b). These exposed nanospheres on the inside and/or outside surfaces of the nanotubes are favorable for lithium ion diffusion from different orientations and provide sufficient contact between active materials and electrolytes.[11,12] The obtained nanomaterials retained their morphology after acid treatment (Fig. S1†).

Transmission electron microscopy (TEM) analyses were employed to characterize the prepared nano-materials. Fig. 3a shows that the product has a nanotube structure and Ni nanoparticles with ~15 nm diameter are decorated homogeneously on the amorphous carbon nanotube. The HRTEM micrograph in Fig. 3b reveals the structure

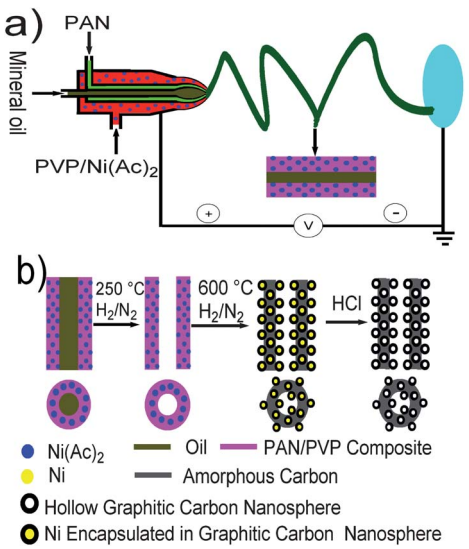

Fig. 1 (a) Schematic illustration of the novel triple-coaxial electrospinning technique used to prepare the PVP/$Ni(Ac)_2$/PAN@Oil coaxial composite nanofibers. (b) Proposed synthesis scheme for ACNHGCNs.

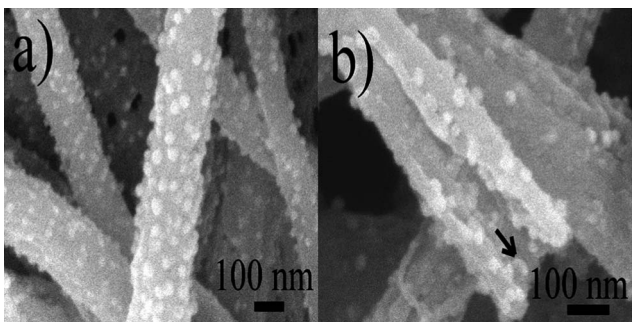

Fig. 2 FESEM images of (a) ACNNNGCNs and (b) broken ACNNNGCNs fabricated by the novel triple-coaxial electrospinning technique.

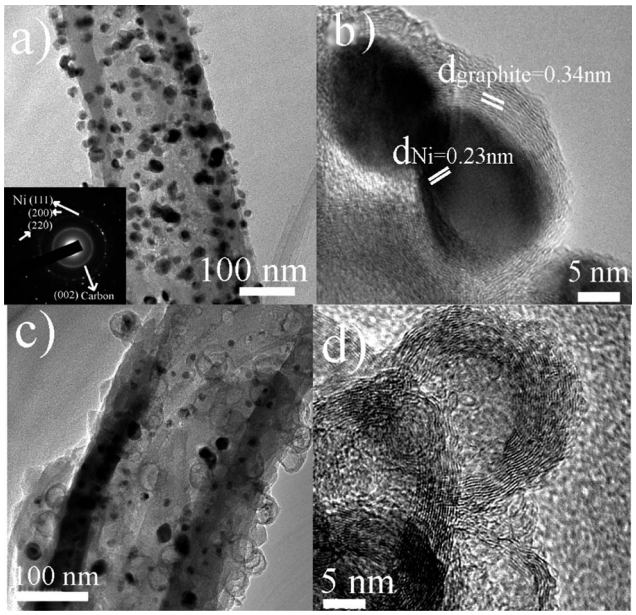

Fig. 3 TEM and HRTEM images of the composite nanotubes (a and b) before and (c and d) after the dissolution of nickel. The inset image shows the SAED pattern of the corresponding nanotubes.

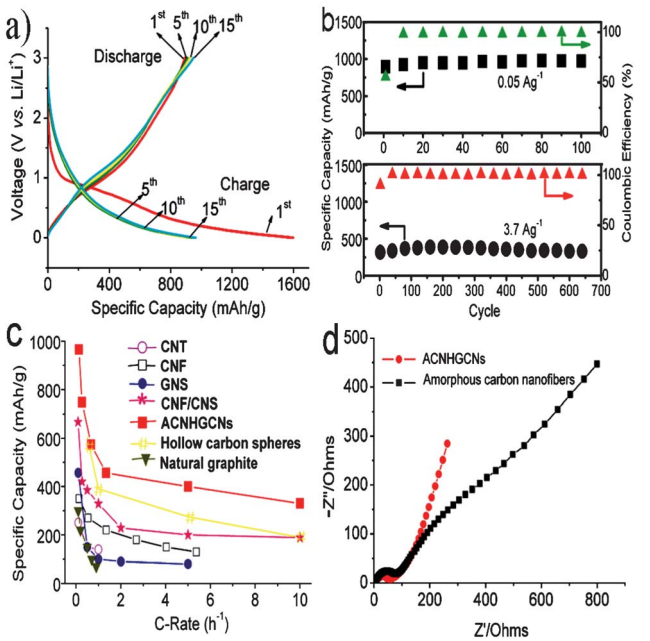

Fig. 4 Electrochemical properties of ACNHGCNs as anode electrodes for Li ion batteries. (a) Charge–discharge voltage profiles of ACNHGCN electrodes cycled at a current density of 50 mA g^{-1} between 3 and 0 V *versus* Li^+/Li. (b) Cycling performance of ACNHGCN electrodes at different current densities. (c) Comparison of the rate capabilities of ACNHGCNs, CNF,[25] CNT,[8] GNS,[13] GNS/CNF,[12] natural graphite[31] and hollow carbon nanospheres.[11] (d) Nyquist plots of ACNHGCNs and amorphous carbon nanofiber electrodes after 10 cycles at a rate of 0.05 A g^{-1}.

of metallic Ni nanoparticles encapsulated in graphitic carbon nano-spheres with a thickness of ~5 nm. The resolved inter-planar distances are ~0.23 and 0.34 nm, which correspond to the (010) plane of Ni and the (002) plane of carbon, respectively. The spot- and ring-like patterns in the selected area electron diffraction (SAED) (inset in Fig. 3a), energy dispersive X-ray spectroscopy (EDS) (Fig. S2†), and X-ray diffraction (XRD) (Fig. S3†) further confirm the presence of crystalline Ni and carbon. The inside diameters of the nanotubes were measured to be ~80 nm. After acid treatment, the metallic Ni nanoparticles were dissolved, leading to the formation of hollow graphitic carbon nano-spheres with a diameter of ~15 nm (Fig. 3c and d). According to the FESEM and HRTEM images (Fig. 2, 3 and S4†), the walls of the amorphous carbon nanotubes partly consist of hollow graphitic carbon nanospheres, some are decorated on the inside and outside surfaces. Raman spectrum analyses revealed that the obtained nanomaterials were partly graphitic carbon (Fig. S5†). Although the small dark Ni particles still can be seen in the ACNHGCNs, its concentration of ~1.6 wt% obtained by EDS (Fig. S6†) is too small to have any significant effect on the specific capacity of ACNHGCNs.

Fig. 4a shows the galvano-static voltage profiles of ACNHGCNs at a current density of 50 mA g^{-1} in the voltage range 0–3 V *versus* Li^+/Li. The voltage plateau at ~0.7 V in the first discharge cycle is closely related to the electrolyte decomposition and formation of a solid electrolyte interface (SEI).[7] The first charge and discharge specific capacities are 1597 and 892 mA h g^{-1}, respectively. The large irreversible capacity in the initial cycle can be ascribed to the SEI formation.[23] The specific capacity approaches an optimized value of 969 mA h g^{-1} after the 15th cycle, which is higher than that of earlier cycles. This result is because of the fact that it is harder for the binder to soak and absorb the electrolyte. The hollow nanospheres were not fully activated during the initial cycles, but the lithium-ion transport channel was extended as the charge–discharge cycling progressed, which activated the remainder of the carbon.[24] Fig. 4b shows that the ACNHGCNs exhibited good cyclic performance and maintained a reversible capacity of ~965 mA h g^{-1} after 100 cycles, whereas ACNNGCNs and amorphous carbon retained only 531 and 400 mA h g^{-1}, respectively (Fig. S7 and S8† for the structure of amorphous carbon). To the best of our knowledge, this performance is superior to that of other carbon materials including carbon nanofibers (CNF, 200 mA h g^{-1}),[25] carbon nanotubes (CNT, 210 mA h g^{-1}),[8] CNF/CNT (546 mA h g^{-1}),[26] electrospun porous amorphous CNF (~530 mA h g^{-1})[27] and graphene (453 mA h g^{-1}),[12] as well as metal oxides and their composites such as Mn_3O_4–graphene (890 mA h g^{-1}),[28] MnO_2–CNT (~700 mA h g^{-1})[29] and SnO_2 (559 mA h g^{-1}).[30] Furthermore, the capacity of ~330 mA h g^{-1} at 3.7 A g^{-1} is retained after 650 cycles, and the coulombic efficiencies at both low and high current density remain more than 99% after the initial few cycles. Fig. S9† shows the cyclic voltammograms of the ACNHGCN electrode at 0.1 mV s^{-1}. It is clearly shown that there are two reduction peaks of ~1.5 V and 0.7 V in the first cycle, which correspond to the irreversible reactions between the ACNHGCN electrode and electrolyte, and the co-intercalation of the solvated lithium ion into graphene sheets.[12,31] The change from the first cycle to the second cycle is due to the incomplete conversion reaction and irreversible lithium loss because of the formation of the SEI film.[31] During the second cycle to the fourth cycle, there is no clear change implying that the electrode is stable during the following charge–discharge cycles after the first cycle. Furthermore, there are not any peaks in the CV corresponding to reduction–oxidation reactions of NiO/Ni.[32] This also indicates that the Ni particles with a content of ~1.6 wt% in ACNHGCNs have a very small contribution to the capacity of the electrode. Therefore, the high capacity should be mainly due to

the ACNHGCNs. Fig. 4c shows the rate capability of the ACNHGCN electrode. At current densities of 0.05, 0.1, 0.25, 0.5, 1.85 and 3.7 A g^{-1}, the reversible capacities of ACNHGCNs are about 960, 748, 573, 456, 400 and 330 mA h g^{-1}, respectively, which are higher than those of CNF,[25] CNT,[8] graphene sheets (GNS),[13] GNS/CNF,[12] natural graphite[33] and hollow carbon nanospheres.[11] Electrochemical impedance spectroscopy (EIS) measurements also showed that the value of high-frequency semicircle in ACNHGCNs is much smaller than in amorphous carbon nanofibers, implying that the ACNHGCN electrodes possess a higher electrical conductivity and a more rapid charge-transfer reaction for lithium ion insertion and extraction (Fig. 4d).[11,12] These show that ACNHGCNs have a good cycling stability at both low and high current density and outstanding rate performance. To demonstrate potentials for real battery application we have measured the volumetric capacities of the ACNHGCNs as shown in Fig. S10†. It is shown that the ACNHGCNs exhibit a high volumetric capacity of ~1.42 A h cm^{-3} which is approximately 1.7 times higher than that of graphite (0.837 A h cm^{-3})[34] and maintain excellent reversible volumetric capacity over 100 cycles. We will further study the tap density of ACNHGCNs by adjusting the diameter of ACNHGCNs *via* an electrospinning process and decorating the ACNHGCNs with other materials to obtain even higher volumetric capacities.

To better understand the reasons that ACNHGCN electrodes exhibited very high specific capacity, we further used HRTEM to examine the structural change of the hollow graphitic carbon nanospheres (HGCNs) upon the electrochemical charge–discharge process (Fig.5). Fig. 5a shows that the wall of a hollow graphitic carbon nanosphere contains many defects between discontinuous graphene sheets, as indicated by the arrows. Also, the hollow structure would provide additional sites for Li^+ storage after dissolving Ni nanoparticles. The defects and the hollow structure give extra sites for storage of lithium ions, thereby greatly enhancing the electrode capacity.[23,35–37] The morphology of the HGCN becomes a little vague and the crystallinity decreases after the initial 5 charge–discharge cycles (Fig. 5b). This effect is clearer for the HGCN after stabilization following 100 charge–discharge cycles (Fig. 5c), and is confirmed by Raman scattering (Fig. S11†). Fig. 5d further demonstrates that the pore size of HGCN on ACNHGCNs is ~15 nm. The two peaks between 1 and 5 nm indicate the existence of nano-pores in the wall of the amorphous carbon nanotubes due to the calcination of electrospun composite precursors since ACNNNGCNs also show two similar types of pore sizes between 1 and 5 nm when compared to amorphous carbon nanofibers (Fig. S12†). These results show that the HGCN as well as nanopores in the wall of nanotubes have more sites for the storage of lithium ions, yielding much increased specific capacity.[23,35–37]

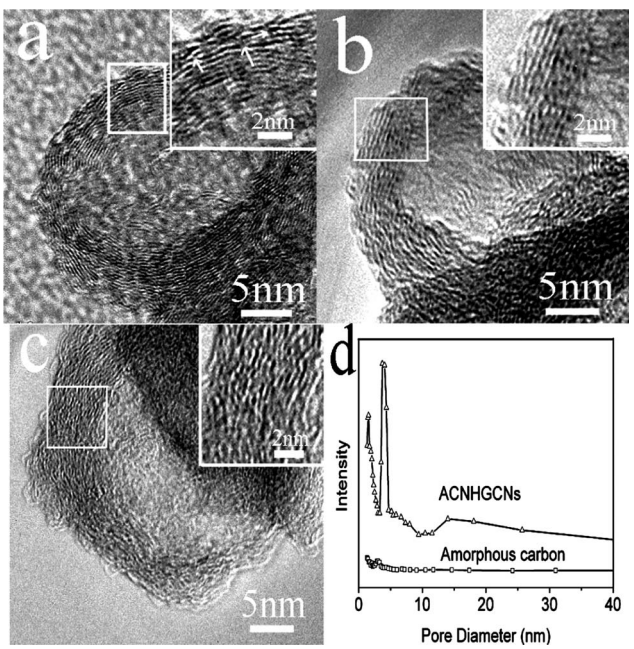

Fig. 5 HRTEM images of hollow graphitic carbon nanosphere electrodes: (a) before and after (b) 5, and (c) 100 charge–discharge cycles. (d) Pore size distribution of ACNHGCNs and amorphous carbon calculated using the BJH method.

Given its superior electrochemical performance and good combination of a high reversible capacity, excellent cycle stability and remarkable rate capability, the ACNHGCN electrode is a very promising candidate anode material for the next generation LIBs. The electrochemical enhancement would be attributed to the unique structure of ACNHGCNs, which yields several favorable properties. First, the defects in the hollow walls, the hollow structure, and nanopores in the wall of tubes provide extra sites for the storage of Li^+, which improve the lithium-storage capacity.[23,35–37] Second, the hollow nanospheres, nanopores and nanotube core act as buffers to substantially withstand the large volume expansion and shrinkage that occur during the Li insertion and extraction process, increasing the cycle lifetime of the electrode.[15] Third, the structures of the hollow nanospheres and nanochannel nanotubes and nanopores allow better Li^+ access and fast transportation of lithium ions, thus reducing substantially the diffusion paths for Li^+.[16–18] Finally, the architecture maintains the mechanical integrity and high electrical conductivity of the overall electrode. All these characteristics enhance the rate performance of ACNHGCNs.

Conclusions

In summary, we have successfully employed a novel triple-coaxial electrospinning technique to prepare a novel architecture consisting of amorphous carbon nanotubes decorated with hollow graphitic carbon nanospheres. The obtained nanomaterials exhibited excellent electrochemical performance, with a good combination of high specific discharge capacity and volumetric capacity, good cycling stability and rate capability, which makes them excellent candidates for use as anode materials for the next-generation high power and high energy LIBs.

Acknowledgements

The authors are grateful for the support received from the Research Grant Council of the Hong Kong Special Administration Region (grant: PolyU 5349/10E) and The Hong Kong Polytechnic University (grant: 1-BD08).

Notes and references

1 P. Poizot and F. Dolhem, *Energy Environ. Sci.*, 2011, **4**, 2003.
2 V. Etacheri, R. Marom, R. Elazari, G. Salitra and D. Aurbach, *Energy Environ. Sci.*, 2011, **4**, 3243.

3 Y. S. Hu, P. Adelhelm, B. M. Smarsly, S. Hore, M. Antonietti and J. Maier, *Adv. Funct. Mater.*, 2007, **17**, 1873.
4 N. A. Kaskhedikar and J. Maier, *Adv. Mater.*, 2009, **21**, 2664.
5 S. S. Zhang, *J. Power Sources*, 2006, **161**, 1385.
6 K. D. Shyamal, P. Manu and J. B. Aninda, *ACS Appl. Mater. Interfaces*, 2010, **2**, 2091.
7 D. Deng and J. Y. Lee, *Chem. Mater.*, 2007, **19**, 4198.
8 A. S. Claye, J. E. Fischer, C. B. Huffman, A. G. Rinzler and R. E. Smalley, *J. Electrochem. Soc.*, 2000, **147**, 2845.
9 J. M. Shen and Y. T. Feng, *J. Phys. Chem. C*, 2008, **112**, 13114.
10 C. N. R. Rao, A. K. Sood, K. S. Subrahmanyam and A. Govindaraj, *Angew. Chem., Int. Ed.*, 2009, **48**, 7752.
11 S. Yang, X. L. Feng, L. J. Zhi, Q. Cao, J. Maier and K. Mullen, *Adv. Mater.*, 2010, **22**, 838.
12 Z. J. Fan, J. Yan, T. Wei, G. Q. Ning, L. J. Zhi, J. C. Liu, D. X. Cao, G. L. Wang and F. Wei, *ACS Nano*, 2011, **5**, 2787.
13 E. Yoo, J. Kim, E. Hosono, H. Zhou, T. Kudo and I. Honma, *Nano Lett.*, 2008, **8**, 2277.
14 T. Bhardwaj, A. Antic, B. Pavan, V. Barone and B. D. Fahlman, *J. Am. Chem. Soc.*, 2010, **132**, 12556.
15 X. Wang, L. J. Zhi, N. Tsao, Z. Tomovic, J. L. Li and K. Mullen, *Angew. Chem., Int. Ed.*, 2008, **47**, 2990.
16 E. McRae and J. F. Mareche, *J. Mater. Res.*, 1988, **3**, 75.
17 A. R. Ubbelohde, *Carbon*, 1976, **14**, 1.
18 R. C. Vickery and N. L. Campbell, *J. Am. Chem. Soc.*, 1957, **79**, 5897.
19 S. M. Shang, X. M. Yang and X. M. Tao, *Polymer*, 2009, **50**, 2815.
20 A. Thess, R. Lee, P. Nikolaev, H. J. Dai, P. Petit, J. Robert, C. H. Xu, Y. H. Lee, S. G. Kim, A. G. Rinzler, D. T. Colbert, G. E. Scuseria, D. Tománek, J. E. Fischer and R. E. Smalley, *Science*, 1996, **273**, 483.
21 D. Li and Y. N. Xia, *Nano Lett.*, 2004, **4**, 933.
22 Y. S. Zhou, D. Z. Yang, X. M. Chen, Q. Xu, F. M. Lu and J. Nie, *Biomacromolecules*, 2008, **9**, 349.
23 E. Peled, C. Menachem, D. BarTow and A. Melman, *J. Electrochem. Soc.*, 1996, **143**, L4.
24 C. C. Li, X. M. Yin, L. B. Chen, Q. H. Li and T. H. Wang, *J. Phys. Chem. C*, 2009, **113**, 13438.
25 H. Habazaki, M. Kiriu and H. Konno, *Electrochem. Commun.*, 2006, **8**, 1275.
26 J. Zhang, Y. S. Hu, J. P. Tessonnier, G. Weinberg, J. Maier, R. Schlögl and D. S. Su, *Adv. Mater.*, 2008, **20**, 1450.
27 L. W. Ji and X. W. Zhang, *Electrochem. Commun.*, 2009, **11**, 684.
28 H. L. Wang, L. F. Cui, Y. Yang, H. S. Casalongue, J. T. Robinson, Y. Y. Liang, Y. Cui and H. J. Dai, *J. Am. Chem. Soc.*, 2010, **132**, 13978.
29 A. L. M. Reddy, M. M. Shaijumon, S. R. Gowda and P. M. Ajayan, *Nano Lett.*, 2009, **9**, 1002.
30 C. Wang, Y. Zhou, M. Y. Ge, X. B. Xu, Z. L. Zhang and J. Z. Jiang, *J. Am. Chem. Soc.*, 2010, **132**, 46.
31 Y. K. Choi, K. I. Chung, W. S. Kim and Y. E. Sung, *Microchem. J.*, 2001, **68**, 61.
32 X. H. Wang, Z. B. Yang, X. L. Sun, X. W. Li, D. S. Wang, P. Wang and D. Y. He, *J. Mater. Chem.*, 2011, **21**, 9988–9990.
33 H. L. Zhang, Y. Zhang, X. G. Zhang, F. Li, C. Liu, J. Tan and H. M. Cheng, *Carbon*, 2006, **44**, 2778.
34 S. Iwamura, H. Nishihara and T. Kyotani, *J. Phys. Chem. C*, 2012, **116**, 6004.
35 A. Mabuchi, *Tanso*, 1994, **165**, 298.
36 K. Tatsumi, J. Conard, M. Nakahara, S. Menu, P. Lauginie, Y. Sawada and Z. Ogumi, *Chem. Commun.*, 1997, 687.
37 C. Menachem, E. Peled, L. Burstein and Y. Rosenberg, *J. Power Sources*, 1997, **68**, 277.

